Article

Characterization of Umami Dry-Cured Ham-Derived Dipeptide Interaction with Metabotropic Glutamate Receptor (mGluR) by Molecular Docking Simulation

Alejandro Heres [ORCID], Fidel Toldrá [ORCID] and Leticia Mora *[ORCID]

Instituto de Agroquímica y Tecnología de Alimentos (CSIC), Avenue Agustín Escardino 7, 46980 Paterna, Spain; alejandergo@iata.csic.es (A.H.); ftoldra@iata.csic.es (F.T.)
* Correspondence: lemoso@iata.csic.es; Tel.: +34-963900022

Abstract: Dry-cured ham-derived dipeptides, generated along a dry-curing process, are of high importance since they play a role in flavor development of dry-cured ham. The objective of this study was to analyze the residues of the less-studied metabotropic glutamate receptor 1 (mGluR1) implicated in the recognition of umami dry-cured ham dipeptides by molecular docking simulation using the AutoDock Suite tool. AH, DA, DG, EE, ES, EV, and VG (and glutamate) were found to attach the enzyme with inhibition constants ranging from 12.32 μM (AH) to 875.75 μM (ES) in the case if *Rattus norvegicus* mGluR1 and 17.44 μM (VG) to 294.68 μM (DG) in the case of *Homo sapiens*, in the open–open conformations. Main interactions were done with key receptor residues Tyr74, Ser186, Glu292, and Lys409; and Ser165, Ser186, and Asp318, respectively, for the two receptors in the open–open conformations. However, more residues may be involved in the complex stabilization. Specifically, AH, EE and ES relatively established a higher number of H-bonds, but AH, EV, and VG presented relatively lower Ki values in all cases. The results obtained here could provide information about structure and taste relationships and constitute a theoretical reference for the interactions of novel umami food-derived peptides.

Keywords: dry-cured ham; dipeptides; flavor; umami: mGluR1

1. Introduction

Dry-cured ham is a high added-value product consumed worldwide [1,2]. The European Union recognizes a broad variety of different dry-cured ham types, half of which are classified as protected designation of origin and half classified as protected geographical indication [3], due to the particular pig breed and processing conditions that influence the final texture and flavor characteristics of the product. The dry-curing process is crucial for the quality of the product, which is conditioned by a wide range of factors such as animal feedstuffs, raw material and pork genetics, age, sex, and processing conditions, since they have an effect on the biochemical reactions that arise from the post-mortem stage [3–8]. Proteolysis and lipolysis are two of the main biochemical reactions contributing to the organoleptic properties. The endogenous exopeptidases and endopeptidases cleave muscle proteins, mainly myofibrillar and sarcoplasmic proteins, leading to the release of high amounts of short peptides and amino acids by which the sensory profiles of dry-cured ham are strongly affected [9,10]. Many peptides generated in dry-cured ham have been identified and characterized, some of which exert a wide range of bioactivities [11]. However, little is known about their role as taste-active compounds. In this line, size-exclusion peptide fractionation demonstrated that bitterness was perceived in the earlier-running fractions of molecular mass, around 1700 Da, followed by savory and salty taste from 1700 to 1500 Da. Umami and "brothy" tastes were perceived below 1500 Da, and finally bitter taste was found again due to the presence of Y and hypoxanthine amino acids. Hydrolysis of the savory fractions showed that G, K, S, taurine, T, A, P, Y, V, M, I, and L amino acids

were the most abundant in comparison with the lowest levels of C amino acid/cystine. The hydrolyzed umami and brothy fraction revealed a high content in F amino acid, whose bitter taste was (pointed out to be) masked by the levels of E, S, G, H, A, M, and K amino acids [12]. Precisely, it was discovered that the response to bitterness can be suppressed by acidic dipeptides EE, DD, and amino acids E and D [13]; in agreement with umami peptides ED, EE, ES, DES, and EGS, they also behave as bitterness suppressors [14]. In another study with a similar methodology, fractions below 1200 Da were related with sour, bitter, and salty tastes, in joint, with brothy and dry-cured ham typical aromatics. It was also found that those tastes discovered in some fractions may be due to the presence of dipeptides, such as VE, IV, LE, ID, AM, GE, ER, PL, GS, DV, and SK [15]. These findings constitute interesting results about the relation of the peptide size and flavor, as well as the potential flavor characteristics of some dipeptides, but there are still limited data about the specific taste, which is imparted by isolated peptides. Data obtained from in silico simulations provide insight into the potential taste and interaction mechanism with the taste receptors. Examples of studies following molecular docking allowed the discovery of pharmaceutical and bioactive compounds [16], such as SFGYVAE, a potent inhibitory peptide for 3-hydroxy-3-methylglutaryl CoA reductase [17]; molecules approved in phase-I clinical trials to identify 3CL protease inhibitors to treat COVID-19 [18]; or a methodology for developing new neuroprotective drugs from traditional Chinese medicine, which target metabotropic umami receptors (mGluRs) [19], demonstrating that in silico analyses streamline the empirical research. Indeed, the details obtained from database searches can be used for the formation of a data matrix when constructing a quantitative structure–activity relationship biostatistical model, and for molecular docking to predict the potential taste of unknown peptides by estimating the receptor's residues involved in the interaction and the binding affinities [20,21].

Specialized taste receptor cells harbor G protein-coupled receptors (GPCRs), whose signalization when binding to umami substances is transmitted to gustatory afferent fibers via ATP signaling [22,23]. To date, the known umami receptors are T1R1/T1R3, expressed in the taste cells of the lingual epithelium and in the gut [24], mGluR4, also expressed in the brain [25], and mGluR1, also widely expressed throughout the central nervous [26] and in the stomach [27]. Although the heterodimer receptor T1R1/T1R3 was identified as one of the most firmly established umami receptors [28], intriguingly, knockout mice lacking the *Tas1r1* or *Tas1r3* gene sequences showed only partial taste loss for the umami taste, evidence arguing that mGluR1 receptors can also contribute to the umami taste [26,29,30]. Unfortunately, a structure of T1R1/T1R3 has not been published to date, and while homology models based on mGluR1 atomic coordinates have been used for the study of T1R1/T1R3 interactions with umami compounds, less is known about how mGluR1 recognizes such taste-active molecules.

The present work is aimed to, in silico, predict the interactions, by using *Rattus norvegicus* and *Homo sapiens* mGluR1 receptors, the latter more recently disclosed, with umami dry-cured ham-derived dipeptides recently identified, and which could have a key role in the development of dry-cured ham flavor. The findings obtained here would serve as a reference for potential mGluR1-interacting peptides susceptible to imparting the umami taste, as well as serve as a theoretical insight into the umami-contributing peptide sequences.

2. Materials and Methods

The dipeptides AH (PubChem ID: 9837455), DA (PubChem ID: 5491963), DG (PubChem ID: 151148), EE (PubChem ID: 439500), ES (PubChem ID: 6995653), EV (PubChem ID: 6992567), VG (PubChem ID: 6993111), which have been described as taste-related peptides and are present in dry-cured ham, were processed for an in silico analysis in order to predict their potential interacting mechanisms with the receptor. The ligand sequences, as well as that from glutamate (E) (PubChem ID: 33032), were obtained in "sdf" format from PubChem tool (https://pubchem.ncbi.nlm.nih.gov/, accessed on 15 July 2021) [31],

and the PDB files were extracted using Discovery Studio Visualizer v20.1.0.19295 software (Dassault Systèmes BIOVIA Corp., 2020). The structures of mGluR1 *Rattus norvegicus* closed–open and open–open conformations, and *Homo sapiens* open–open conformation (protein data bank ID: 1EWK, 1EWT and 3KS9), in complex with E [32], ligand free and LY341495 antagonist [33], respectively, were downloaded from the Protein Databank (PDB) tool (https://www.rcsb.org/, accessed on 15 July 2021) [34].

Ligand-protein docking simulations were carried out using AutoDock v1.5.6 and AutoDock v4.2.5.1 (Scripps Research Institute) software [35,36]. The minimum system requirements are Intel 32/64-bit, Pentium/Dual core, Microsoft Windows (98, 2000, XP, Vista, Windows 7)/Linux and Macintosh, 256 MB of minimum RAM, and 200 MB of minimum hard disk space.

Gasteiger charges and hydrogens were added to all molecules; water molecules and original ligands were also removed from the enzyme, and ligand torsions were detected by AutoDock. Structure data files were converted into the Protein Data Bank partial charge and atom type format.

Firstly, a preliminary test to obtain more information about the coordinates of the area for screening was carried out. Insights were made by submitting the original receptor PDB archives to ProteinsPlus, and processing the molecule with the tool PoseView (https://proteins.plus/, accessed on 15 July 2021) [37,38] and the web server DoGSiteScorer (https://proteins.plus/, accessed on 15 July 2021) [39].

The definitive Grid Box ($60 \times 60 \times 60$) was centered on one of the mGluR1 binding sites where active residues located, with coordinates X = 11,407, Y = 13,031, and Z = 12,342 for 1EWK [40,41], X = 16,958, Y = 28,615, and Z = 45,202 for 1EWT and X = −41,815, Y = 9345 and Z = 34,170 for 3KS9 [42], with a spacing of 0.375 Å. Fifty docking runs were performed, using a Lamarckian genetic algorithm between the flexible ligand and rigid receptor, a population size of 150, a maximum of 2,500,000 generations and 2,500,000 evaluations for 50 GA runs. The root-mean-square deviation tolerance was set to 2.0 Å for the clustering of docking results. Analysis of the results were conducted by sorting the different complexes with respect to the predicted binding energy. The pose with the lowest binding energy in each case was individually examined, and interactions were processed with online software, Protein–Ligand Interaction Profiler (PLIP) (https://plip-tool.biotec.tu-dresden.de/plip-web/plip/index, accessed on 15 July 2021) [43], to validate the interactions; and with ProteinsPlus (https://proteins.plus/, accessed on 15 July 2021) [37,44] to obtain the two-dimensional representations by using the PoseView algorithm [44].

3. Results and Discussion
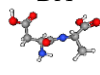
Dipeptides in dry-cured ham are mainly generated by dipeptidyl dipeptidases (DPPs) and by the progressive shortening of longer peptides by other endogenous enzymes. It has been shown that DPPs release dipeptides from the N-terminal of peptide fragments [45], and despite their substrate specificities, all of them are able to release other dipeptides at lower rates [46].

Short peptides are in the limit of some standard proteomic approaches due to their small sizes and signal inhibition, due to matrix interactions in the mass spectrometers [45,47,48]. Considering the high probability of the dipeptides sequence being represented in a wide variety of proteins, the profiling, structural estimation, quantification, and identification using traditional procedures based on matching the *m/z* spectrum with theoretical peptide sequences using databases is not feasible [49,50]. In fact, the de novo interpretation of the fragmented spectra by experienced personnel is frequently needed [48], which is a time-consuming and complex task. Thus, peptidomic approaches based on prior chromatographic steps have been developed to concentrate and isolate those peptides of interest. As a result, umami dipeptides AH, DA, DG, EE, ES, EV, and VG, described in Table 1, have been successfully detected in dry-cured hams. In fact, the dipeptide AH has been identified in Jinhua ham with a relative peak area percentage of 3.40, by size-exclusion chromatography (SEC)-reverse-phase high performance liquid chromatography

(RP-HPLC) coupled with MALDI SYNAPT-multiple monitoring reactions (MRM)-Q-ToF mass spectrometry [51–53].

Table 1. Main physicochemical characteristics attributed to the dipeptides under study.

Dipeptide [a]	Dry-Cured Ham Parental Protein [b]	Net Charge (Value (pI)) [c]	Hydrophobicity [d]	Steric Hindrance [d]	Main Residue Attribute (N-residue, C-residue) [c]
AH	Unknown	0.1 (7.88)	−0.08	0.26	aliphatic, basic
DA	MLC1 [54]	−1 (0.69)	-0.23	0.64	acidic, aliphatic
DG	Unknown	−1 (0.68)	−0.28	0.72	acidic, aliphatic
EE	TTN [55] MLC1 [54]	−2 (0.85)	−0.62	0.68	acidic, acidic
ES	Unknown	−1 (1.01)	−0.44	0.60	acidic, polar
EV	Unknown	−1 (0.94)	−0.04	0.69	acidic, aliphatic
VG	Unknown	0 (3.59)	0.35	0.69	aliphatic, aliphatic
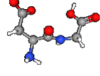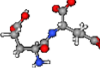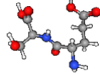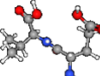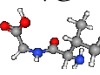
[a] Peptide sequences are given in one-letter code. [b] Known parental protein of origin, MLC1: myosin light chain 1; TTN; titin. [c] Net charges at pH 7, pI values, and main residue attribute obtained from PepCalc (https://pepcalc.com/) (accessed on June 2020). [d] Hydrophobicity and steric hindrance values obtained from ToxinPred [56].

3.1. Rattus Norvegicus and Homo sapiens mGluR1s Shared Homology

The aim of this work was to estimate the interactions between mGluR1 and umami dipeptides found in dry-cured ham. These findings, in joint with peptidomic and further sensory analysis, will provide interesting evidence about the development of dry-cured ham flavor by the generation of short peptides, and will contribute to predict the taste of unknown peptides present in foods. As the *Homo sapiens* mGluR1 crystal structure (PDB ID: 3KS9; UniProt ID: Q13255) was recently resolved, and there is little information about its mechanism, a first comparative study with the most frequently employed *Rattus norvegicus* mGluR1 (PDB ID: 1EWK; UniProt ID: P23385) was conducted. Figure 1 indicates an alignment [57] of both FASTA sequences.

```
P23385 GRM1_RAT        1  MVRLLLIFFPMIFLEMSILPRMPDRKVLLAGASSQRSVARMDGDVIIGALFSVHHQPPAE    60
Q13255 GRM1_HUMAN      1  MVGLLLFFFPAIFLEVSLLPRSPGRKVLLAGASSQRSVARMDGDVIIGALFSVHHQPPAE    60
                          ** ***:*** ****:*:*** *.*************************************

P23385 GRM1_RAT       61  KVPERKCGEIREQYGIQRVEAMFHTLDKINADPVLLPNITLGSEIRDSCWHSSVALEQSI   120
Q13255 GRM1_HUMAN     61  KVPERKCGEIREQYGIQRVEAMFHTLDKINADPVLLPNITLGSEIRDSCWHSSVALEQSI   120
                          ************************************************************

P23385 GRM1_RAT      121  EFIRDSLISIRDEKDGLNRCLPDGQTLPPGRTKKPIAGVIGPGSSSVAIQVQNLLQLFDI   180
Q13255 GRM1_HUMAN    121  EFIRDSLISIRDEKDGINRCLPDGQSLPPGRTKKPIAGVIGPGSSSVAIQVQNLLQLFDI   180
                          ****************:********:***********************************

P23385 GRM1_RAT      181  PQIAYSATSIDLSDKTLYKYFLRVVPSDTLQARAMLDIVKRYNWTYVSAVHTEGNYGESG   240
Q13255 GRM1_HUMAN    181  PQIAYSATSIDLSDKTLYKYFLRVVPSDTLQARAMLDIVKRYNWTYVSAVHTEGNYGESG   240
                          ************************************************************

P23385 GRM1_RAT      241  MDAFKELAAQEGLCIAHSDKIYSNAGEKSFDRLLRKLRERLPKARVVVCFCEGMTVRGLL   300
Q13255 GRM1_HUMAN    241  MDAFKELAAQEGLCIAHSDKIYSNAGEKSFDRLLRKLRERLPKARVVVCFCEGMTVRGLL   300
                          ************************************************************

P23385 GRM1_RAT      301  SAMRRLGVVGEFSLIGSDGWADRDEVIEGYEVEANGGITIKLQSPEVRSFDDYFLKLRLD   360
Q13255 GRM1_HUMAN    301  SAMRRLGVVGEFSLIGSDGWADRDEVIEGYEVEANGGITIKLQSPEVRSFDDYFLKLRLD   360
                          ************************************************************

P23385 GRM1_RAT      361  TNTRNPWFPEFWQHRFQCRLPGHLLENPNFKKVCTGNESLEENYVQDSKMGFVINAIYAM   420
Q13255 GRM1_HUMAN    361  TNTRNPWFPEFWQHRFQCRLPGHLLENPNFKRICTGNESLEENYVQDSKMGFVINAIYAM   420
                          *******************************::***************************

P23385 GRM1_RAT      421  AHGLQNMHHALCPGHVGLCDAMKPIDGRKLLDFLIKSSFVGVSGEEVWFDEKGDAPGRYD   480
Q13255 GRM1_HUMAN    421  AHGLQNMHHALCPGHVGLCDAMKPIDGSKLLDFLIKSSFIGVSGEEVWFDEKGDAPGRYD   480
                          ***************************.***********:********************

P23385 GRM1_RAT      481  IMNLQYTEANRYDYVHVGTWHEGVLNIDDYKIQMNKSGMVRSVCSEPCLKGQIKVIRKGE   540
Q13255 GRM1_HUMAN    481  IMNLQYTEANRYDYVHVGTWHEGVLNIDDYKIQMNKSGVVRSVCSEPCLKGQIKVIRKGE   540
                          *************************************:**********************

P23385 GRM1_RAT      541  VSCCWICTACKENEFVQDEFTCRACDLGWWPNAELTGCEPIPVRYLEWSDIESIIAIAFS   600
Q13255 GRM1_HUMAN    541  VSCCWICTACKENEYVQDEFTCKACDLGWWPNADLTGCEPIPVRYLEWSNIESIIAIAFS   600
                          **************:*******:***********:***************:*********

P23385 GRM1_RAT      601  CLGILVTLFVTLIFVLYRDTPVVKSSSRELCYIILAGIFLGYVCPFTLIAKPTTTSCYLQ   660
Q13255 GRM1_HUMAN    601  CLGILVTLFVTLIFVLYRDTPVVKSSSRELCYIILAGIFLGYVCPFTLIAKPTTTSCYLQ   660
                          ************************************************************

P23385 GRM1_RAT      661  RLLVGLSSAMCYSALVTKTNRIARILAGSKKKICTRKPRFMSAWAQVIIASILISVQLTL   720
Q13255 GRM1_HUMAN    661  RLLVGLSSAMCYSALVTKTNRIARILAGSKKKICTRKPRFMSAWAQVIIASILISVQLTL   720
                          ************************************************************

P23385 GRM1_RAT      721  VVTLIIMEPPMPILSYPSIKEVYLICNTSNLGVVAPVGYNGLLIMSCTYYAFKTRNVPAN   780
Q13255 GRM1_HUMAN    721  VVTLIIMEPPMPILSYPSIKEVYLICNTSNLGVVAPLGYNGLLIMSCTYYAFKTRNVPAN   780
                          ************************************:***********************

P23385 GRM1_RAT      781  FNEAKYIAFTMYTTCIIWLAFVPIYFGSNYKIITTCFAVSLSVTVALGCMFTPKMYIIIA   840
Q13255 GRM1_HUMAN    781  FNEAKYIAFTMYTTCIIWLAFVPIYFGSNYKIITTCFAVSLSVTVALGCMFTPKMYIIIA   840
                          ************************************************************

P23385 GRM1_RAT      841  KPERNVRSAFTTSDVVRMHVGDGKLPCRSNTFLNIFRRKKPGAGNANSNGKSVSWSEPGG   900
Q13255 GRM1_HUMAN    841  KPERNVRSAFTTSDVVRMHVGDGKLPCRSNTFLNIFRRKAGAGNANSNGKSVSWSEPGG   900
                          *************************************** ********************

P23385 GRM1_RAT      901  RQAPKGQHVWQRLSVHVKTNETACNQTAVIKPLTKSYQGSGKSLTFSDASTKTLYNVEEE   960
Q13255 GRM1_HUMAN    901  GQVPKGQHMWHRLSVHVKTNETACNQTAVIKPLTKSYQGSGKSLTFSDTSTKTLYNVEEE   960
                          *.*****:*:***********************************:**************

P23385 GRM1_RAT      961  DNTPSAHFSPPSSPSMVVHRRGPPVATTPPLPPHLTAEETPLFLADSVIPKGLPPPLPQQ  1020
Q13255 GRM1_HUMAN    961  EDAQPIRFSPPGSPSMVVHRRVPSAATTPPLPSHLTAEETPLFLAEPALPKGLPPPLQQQ  1020
                          ::::    :****.********* * .****** ************: .:********* **

P23385 GRM1_RAT     1021  QPQQPPPQQPPQQPKSLMDQLQGVVTNFGSGIPDFHAVLAGPGTPGNSLRSLYPPPPPPQ  1080
Q13255 GRM1_HUMAN   1021  Q-------QPPPQQKSLMDQLQGVVSNFSTAIPDFHAVLAGPGGPGNGLRSLYPPPPPPQ  1073
                          *       *** * ***********:**.:.:************ ***.************

P23385 GRM1_RAT     1081  HLQMLPLHLSTFQEESISPPGEDIDDDSERFKLLQEFVYE--REGNTEEDELEE-EEDLP  1137
Q13255 GRM1_HUMAN   1074  HLQMLPLQLSTFGEELVSPPADD-DDDSERFKLLQEYVYEHEREGNTEEDELEEEEEDLQ  1132
                          *******:**** ** :***.:* *************:*** ************ ****

P23385 GRM1_RAT     1138  TASKLTPEDSPALTPPSPFRDSVASGSSVPSSPVSESVLCTPPNVTYASVILRDYKQSSS  1197
Q13255 GRM1_HUMAN   1133  AASKLTPDDSPALTPPSPFRDSVASGSSVPSSPVSESVLCTPPNVSYASVILRDYKQSSS  1192
                          :******:*************************************:**************

P23385 GRM1_RAT     1198  TL                                                            1199
Q13255 GRM1_HUMAN   1193  TL                                                            1194
                          **
```

Figure 1. Alignment analysis of protein sequences between *Rattus norvegicus* mGluR1 (PDB ID: 1EWK; UniProt ID: P23385) and *Homo sapiens* mGluR1 (PDB ID: 3KS9; UniProt ID: Q13255). Identity: 94.01%; identical positions: 1130; similar positions: 41. Fully conserved residues are indicated with "*"; conservation between groups of strongly similar properties is labeled with ":"; a "." indicates conservation between groups of weakly similar properties; and a blank space signifies none of the above.

As presented in Figure 1, an identity of 94.01% was estimatedbetween *Rattus norvegicus* mGluR1 (PDB ID: 1EWK) and *Homo sapiens* mGluR1 (PDB ID: 3KS9). Only a few mismatches were found at positions apparently not belonging to key residues of the binding site, suggesting that the motif is evolutionarily conserved [58].

Based on their signal transduction pathways and pharmacological properties, mGluRs have been categorized into three groups: Group I (mGluR1 and mGluR5) are normally stimulatory and associated with phospholipase C activation and second messengers, such as inositol and diacylglycerol production. Group II (mGluR2 and mGluR3) and Group III (mGluR4, mGluR6, mGluR7, and mGluR8) normally inhibit glutamatergic neurotransmission and they are both negatively coupled to adenylyl cyclase [59]. The N terminus of mGluRs comprises a large extracellular E-binding domain and the cytoplasmic C terminus of mGluRs participates in interactions with G proteins [25]. The taste receptor mGluR1 has been found in rat circumvallate and foliate papillae of the posterior tongue, in a truncated form compared to its homologous expressed in the brain. Its activation depends on the disulfide-linked homodimer conformation, and signalization probably occurs through IP3 formation and Ca^{2+} release from intracellular stores, but only at concentrations ≥ 1 mmol E [60]. The bi-lobed protomer architectures flexibly change their domain arrangements to form an "open" or "closed" conformation. Upon agonist binding, the protomer is closed at the cleft between the two ligand-binding sites, conformations, which are referred to as closed and open forms. However, the actual conformation in the physiological state is still unknown [61]. To our knowledge, there is only a structure linked to the Human mGluR1 determined, with an open–open conformation (PDB ID: 3KS9), while the most studied *Rattus norvegicus* mGluR1 structure published to date consists of a closed–open conformation (PDB ID: 1EWK). Other structures from this last publication are an open–open conformation (PDB ID: 1EWT) and a closed–open conformation in the ligand free form (PDB ID: 1EWV) [61,62]. For these reasons, this work strives to bring to light the receptor residues implicated when mGluR1 adopts the active closed–open conformation and, at the same time, perform a comparative study between both open–open forms of mGluR1 belonging to the *Rattus norvegicus* and *Homo sapiens*.

In the case of the more studied *Rattus norvegicus* mGluR1 (PDB ID: 1EWK), the active residues are described to be Tyr74, Arg78, Ser164, Ser165, Ser186, Thr188, Asp208, Tyr236, Glu292, Gly293, Asp318, Arg323, and Lys409 [40,41]. Otherwise, the *Homo sapiens* mGluR1 active residues belonging to the active site have been predicted to be Trp110, Gly163, Ser164, Ser165, Ser186, Tyr236, Asp318, Asp319, Ala329, and Gly379 [42]. Thus, both receptors were evaluated in order to obtain a more accurate prediction.

The dipeptides AH, DA, DG, EE, ES, EV, VG, and glutamic acid (positive control) were studied through molecular docking analyses to understand their possible mechanism of interaction with the umami receptor mGluR1.

3.2. Interaction between Umami Dipeptides and Rattus Norvegicus mGluR1 Closed–Open Conformation

As shown in Table 2 and Figure 2, the estimated interacting residues, binding type, and binding energy of interactions are calculated in this in silico process. It is important to remark that the figures, used for a simpler overview of the dockings, represent two-dimensional interactions obtained from PoseView tool, which estimates the interactions between the complex partners by using simple geometric criteria, such as distances and angles [63]. Thus, not all interactions are drawn.

Table 2. *Rattus norvegicus* closed–open conformation (PDB ID: 1EWK) of mGluR1 residues involved in docking interactions with glutamic acid and the umami dry-cured ham dipeptides of this study, with docking scores.

Ligand	PubChem ID	Binding Energy (kcal/mol)	Inhibition Constant (μM)	Protein Residues Involved in H-Bond Interactions [Chain:Residue (Distance btw Donor-Acceptor) (Protein Donor/Acceptor, Residue from Side Chain)]	No. of H-Bonds	Protein Residues Involved in Hydrophobic Interactions [Chain:Residue (Distance btw Carbon Atoms)]	Protein Residues Involved in Salt Bridges [Chain:Residue (Distance btw Centers of Charge) (Ligand Functional Group Providing the Charge)]
E	33,032	−6.56	15.58	A:**Tyr74** (2.80 Å) (Donor,sd) A:**Tyr74** (2.89 Å) (Acceptor,sd) A:**Ser165** (3.03 Å) (Donor) A:**Ser165** (2.86 Å) (Acceptor,sd) A:**Ser186** (4.08 Å) (Donor,sd) A:**Thr188** (2.80 Å) (Donor) A:**Asp318** (3.47 Å) (Acceptor,sd)	7	*Absent*	A:**Arg323** (5.39 Å) (Carboxilate) A:**Lys409** (3.25 Å) (Carboxilate)
AH	9,837,455	−6.93	8.26	A:**Tyr74** (2.84 Å) (Donor,sd) A:**Tyr74** (2.84 Å) (Acceptor,sd) A:**Ser186** (2.82 Å) (Donor,sd) A:**Ser186** (3.88 Å) (Acceptor,sd) A:**Tyr236** (3.74 Å) (Acceptor,sd) A:**Glu292** (4.02 Å) (Acceptor,sd) A:**Gly293** (3.57 Å) (Donor) A:**Arg323** (2.79 Å) (Donor,sd)	8	A:Trp110 (3.86 Å) A:**Tyr236** (3.27 Å)	A:**Arg78** (4.47 Å) (Carboxilate) A:**Lys409** (3.49 Å) (Carboxilate)
DA	5,491,963	−6.23	27.24	A:**Tyr74** (2.68 Å) (Donor,sd) A:**Ser165** (3.12 Å) (Donor) A:**Ser165** (2.73 Å) (Acceptor,sd) A:**Thr188** (3.16 Å) (Donor) A:**Gly293** (3.06 Å) (Donor) A:**Asp318** (3.44 Å) (Acceptor,sd) A:Gly319 (3.08 Å) (Acceptor) A:**Lys409** (3.69 Å) (Donor,sd)	8	A:**Tyr236** (3.13 Å) A:**Glu292** (3.17 Å)	A:**Arg323** (4.24 Å) (Carboxilate) A:**Lys409** (5.38 Å) (Carboxilate)

Table 2. *Cont.*

Ligand	PubChem ID	Binding Energy (kcal/mol)	Inhibition Constant (μM)	Protein Residues Involved in H-Bond Interactions [Chain:Residue (Distance btw Donor-Acceptor) (Protein Donor/Acceptor, Residue from Side Chain)]	No. of H-Bonds	Protein Residues Involved in Hydrophobic Interactions [Chain:Residue (Distance btw Carbon Atoms)]	Protein Residues Involved in Salt Bridges [Chain:Residue (Distance btw Centers of Charge) (Ligand Functional Group Providing the Charge)]
DG	151,148	−7.12	6.00	A:Tyr74 (3.13 Å) (Acceptor,sd) A:Gly163 (3.73 Å) (Acceptor) A:Ser165 (2.72 Å) (Donor) A:Ser165 (2.77 Å) (Acceptor,sd) A:Ser186 (2.82 Å) (Donor,sd) A:Thr188 (3.05 Å) (Donor) A:Asp318 (3.46 Å) (Acceptor,sd) A:Lys409 (3.90 Å) (Donor,sd)	8	A:Tyr236 (3.48 Å)	A:Arg78 (3.56 Å) (Carboxilate) A:Lys409 (3.97 Å) (Carboxilate)
EE	439,500	5.77	59.42	A:Tyr74 (2.97 Å) (Acceptor,sd) A:Tyr74 (3.22 Å) (Donor,sd) A:Tyr74 (3.22 Å) (Acceptor,sd) A:Ser165 (2.73 Å) (Donor) A:Ser186 (2.76 Å) (Donor,sd) A:Ser186 (2.61 Å) (Acceptor) A:Thr188 (2.99 Å) (Donor) A:Gly293 (3.41 Å) (Donor) A:Met294 (3.14 Å) (Donor) A:Gly319 (2.55 Å) (Acceptor) A:Arg323 (2.44 Å) (Donor,sd)	11	A:Tyr74 (3.33 Å) A:Trp110 (3.10 Å) A:Trp110 (3.51 Å) A:Glu292 (3.54 Å)	A:Arg71 (4.74 Å) (Carboxilate) A:Arg78 (4.28 Å) (Carboxilate) A:Arg323 (4.21 Å) (Carboxilate) A:Lys409 (3.60 Å) (Carboxilate)
ES	6,995,653	−6.87	9.17	A:Tyr74 (3.46 Å) (Donor,sd) A:Tyr74 (3.46 Å) (Acceptor,sd) A:Tyr74 (2.80 Å) (Acceptor,sd) A:Ser166 (2.97 Å) (Donor,sd) A:Gly293 (3.68 Å) (Donor) A:Met294 (3.03 Å) (Donor) A:Asp318 (3.57 Å) (Acceptor,sd) A:Arg323 (2.94 Å) (Donor,sd) A:Arg323 (3.86 Å) (Donor,sd)	9	A:Trp110 (3.12 Å) A:Lys409 (3.84 Å)	A:Arg71 (3.44 Å) (Carboxilate) A:Arg78 (3.72 Å) (Carboxilate) A:Arg323 (4.04 Å) (Carboxilate) A:Lys409 (3.99 Å) (Carboxilate)

Table 2. *Cont.*

Ligand	PubChem ID	Binding Energy (kcal/mol)	Inhibition Constant (μM)	Protein Residues Involved in H-Bond Interactions [Chain:Residue (Distance btw Donor-Acceptor) (Protein Donor/Acceptor, Residue from Side Chain)]	No. of H-Bonds	Protein Residues Involved in Hydrophobic Interactions [Chain:Residue (Distance btw Carbon Atoms)]	Protein Residues Involved in Salt Bridges [Chain:Residue (Distance btw Centers of Charge) (Ligand Functional Group Providing the Charge)]
EV	6,992,567	−6.96	7.87	A:**Tyr74** (3.77 Å) (Acceptor,sd) A:**Tyr74** (3.83 Å) (Donor,sd) A:**Glu292** (3.65 Å) (Acceptor,sd) A:**Glu292** (3.28 Å) (Acceptor,sd) A:**Gly293** (2.85 Å) (Donor) A:Met294 (3.11 Å) (Donor) A:**Asp318** (2.91 Å) (Acceptor,sd) A:**Arg323** (2.55 Å) (Donor,sd)	8	A:Trp110 (3.48 Å) A:**Glu292** (3.03 Å) A:Met294 (3.19 Å)	A:Arg71 (4.49 Å) (Carboxilate) A:**Arg323** (3.19 Å) (Carboxilate) A:**Lys409** (2.69 Å) (Carboxilate)
VG	6,993,111	−8.31	0.811	A:**Tyr74** (2.93 Å) (Acceptor,sd) A:Gly163 (3.57 Å) (Acceptor) A:**Ser186** (2.72 Å) (Donor,sd) A:**Thr188** (3.47 Å) (Acceptor,sd) A:**Lys409** (3.96 Å) (Donor,sd)	5	A:Tyr236 (3.44 Å) A:Tyr236 (3.37 Å)	A:**Arg78** (3.66 Å) (Carboxilate) A:**Lys409** (3.75 Å) (Carboxilate)

Key residues of the binding site are highlighted in bold. Common residues for which glutamate and dipeptides interact are colored in purple.
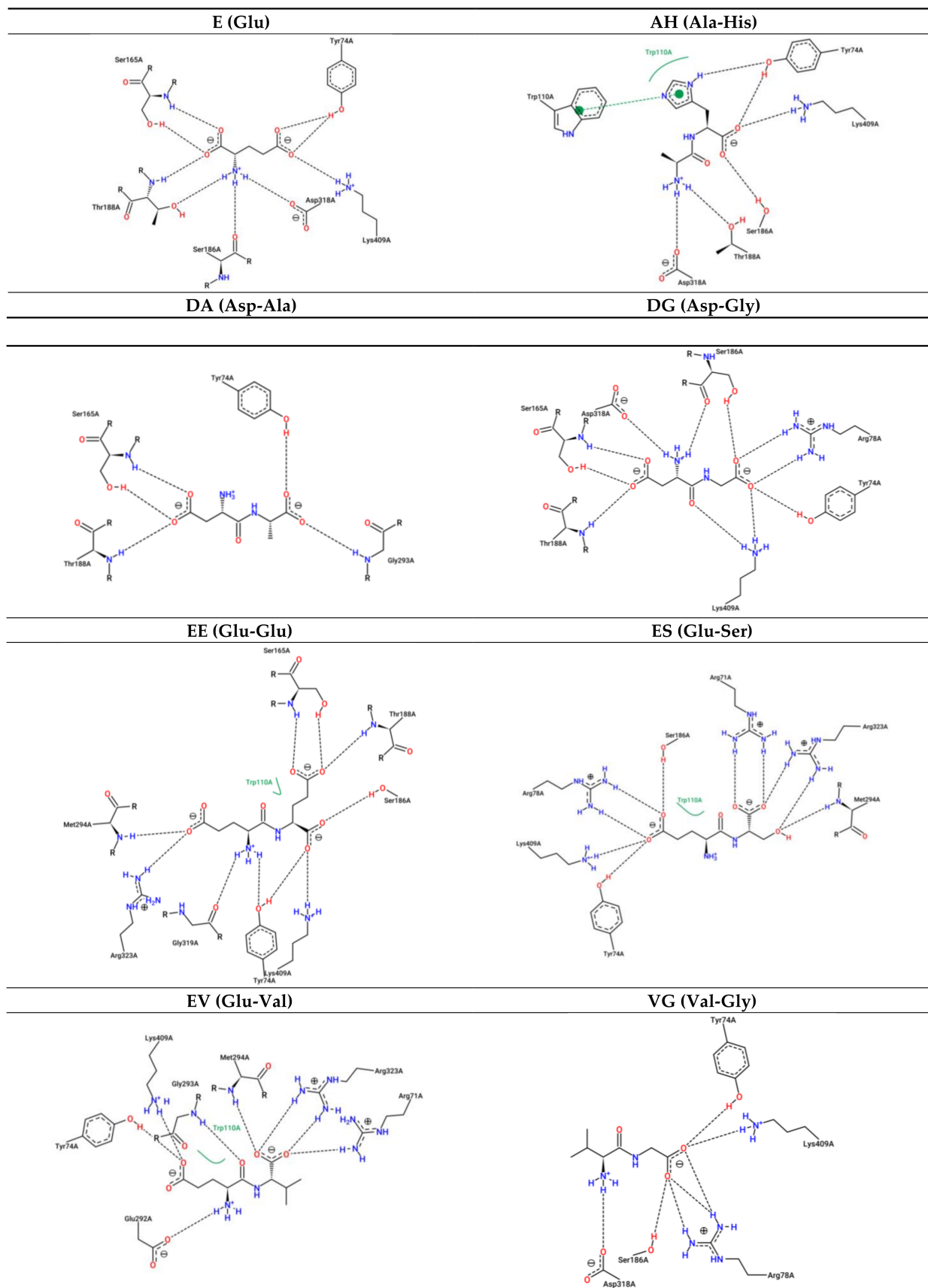
Figure 2. Two-dimensional representation of protein–ligand interactions between *Rattus norvegicus* closed–open

conformation of mGluR1 (PDB ID: 1EWK) and Glu (PubChem ID: 33032), AH (PubChem ID: 9837455), DA (PubChem ID: 5491963), DG (PubChem ID: 151148), EE (PubChem ID: 439500), ES (PubChem ID: 6995653), EV (PubChem ID: 6992567), VG (PubChem ID: 6993111). H bonds are shown as dashed lines, hydrophobic contacts are represented by green splines; the corresponding pocket residues are shown in the same color. Diagrams obtained from the ProteinsPlus PoseView tool, from which E amino acid was predicted to interact with Tyr74, Ser165, Thr188, Ser186, Asp318 and Lys409 by H-bonds; AH, with Tyr74, Ser186, Thr188, Aps318 and Lys409 by H-bonds, Trp110 by π–π stacking and a hydrophobic interaction; DA, with Tyr74, Ser165, Thr188 and Gly293 by H-bonds; DG, with Tyr74, Arg78, Ser165, Ser186, Thr188, Asp318, and Lys409 by H-bonds; EE, with Tyr74, Ser165, Ser186, Thr188, Met294, Gly319, Arg323, and Lys409 by H-bonds and Trp110 by hydrophobic interaction; ES, with Arg71, Tyr74, Arg78, Ser186, Met294, Arg323, and Lys409 by H-bonds and Trp110 by hydrophobic interaction; EV, with Arg71, Tyr74, Glu292, Gly293, Met294, Arg323, and Lys409 by H-bonds and Trp110 by hydrophobic interaction; and VG, with Tyr74, Arg78, Ser186, Asp318, and Lys409 by H-bonds.

Rattus norvegicus mGluR1 key receptor residues from the closed–open conformation, Tyr74, Ser165, Ser186, Thr188, Asp318, Arg323, and Lys409 were predicted to interact with E (Ki = 15.58 μM). With respect to the dipeptide AH (Ki = 8.26 μM), the key residues Tyr74, Arg78, Ser186, Tyr 236, Glu293, Arg323 and Lys409 would be implicated. DA (Ki = 27.24 μM) was calculated to interact with Tyr74, Ser165, Thr188, Tyr236, Glu292, Gly293, Asp318, Arg323, and Lys409, while DG (Ki = 6.0 μM) would react with Tyr74, Arg78, Ser165, Ser186, Thr188, Tyr236, Asp318, and Lys409. On one hand, EE (Ki = 59.42 μM) could bond with Tyr74, Arg78, Ser165, Ser186, Thr188, Glu292, Gly293 Arg323, and Lys409. On the other hand, ES (Ki = 9.17 μM) would be able to form connections with Tyr74, Arg78, Gly293, Asp318, Arg323, and Lys409. EV (Ki = 7.87 μM) was estimated to dock between Tyr74, Glu292, Gly293, Asp318, Arg323, and Lys409. Finally, VG (Ki = 811.24 nM) would bind to Tyr74, Arg78, Ser186, Thr188, and Lys409. Nevertheless, it is important to consider that non-key residues may participate in the stabilization, such as with Trp110, for the case of AH, EE, ES, and EV.

Otherwise, residues, such as Arg323 and Lys409, can make interactions of different nature, as they can stablish H-bonds, hydrophobic forces, or even salt bridges. The majority of the interactions are of H-bond nature, even various with the same residue, such as with Tyr74, Ser165, or Arg323. The dipeptide EE, followed by ES, established the largest number of H-bonds, suggesting the presence of an E residue particularly promotes docking with the receptor in comparison with the other dipeptides. In addition, the nature of the C-terminal of these three dipeptides may provide insights on a polar side chain residue benefits the contact with the receptor. The number of hydrophobic interactions and salt bridges appear very similar between them for each dipeptide, except for glutamic acid, which could not form hydrophobic interactions by itself. Finally, the lowest Ki values were those from VG then DG followed by EV and AH.

3.3. Interaction between Umami Dipeptides and Rattus Norvegicus mGluR1 Open–Open Conformation

Table 3 and Figure 3 are presented hereunder, outlining the interactions in this case.

Table 3. *Rattus norvegicus* open–open conformation (PDB ID: 1EWT) of mGluR1 residues involved in docking interactions with glutamic acid and the umami dry-cured ham dipeptides of this study, with docking scores.

Ligand	PubChem ID	Binding Energy (kcal/mol)	Inhibition Constant (μM)	Protein Residues Involved in H-Bond Interactions [Chain:Residue (Distance btw Donor-Acceptor) (Protein Donor/Acceptor, Residue from Side Chain)]	No. of H-Bonds	Protein Residues Involved in Hydrophobic Interactions [Chain:Residue (Distance btw Carbon Atoms)]	Protein Residues Involved in Salt Bridges [Chain:Residue (Distance btw Centers of Charge) (Ligand Functional Group Providing the Charge)]
E	33,032	−4.31	694.05	A:**Tyr74** (3.31 Å) (Acceptor,sd) A:**Tyr74** (2.97 Å) (Acceptor,sd) A:**Tyr74** (2.57 Å) (Acceptor,sd) A:**Ser186** (3.00 Å) (Donor,sd)	4	A:Trp110 (3.30 Å)	A:**Arg78** (3.91 Å) (Carboxilate) A:**Lys409** (3.90 Å) (Carboxilate) A:**Lys409** (2.49 Å) (Carboxilate)
AH	9,837,455	−6.70	12.32	A:**Tyr74** (3.40 Å) (Acceptor,sd) A:**Tyr74** (2.59 Å) (Acceptor,sd) A:**Gly163** (2.74 Å) (Acceptor) A:**Ser165** (3.43 Å) (Donor) A:**Ser186** (2.99 Å) (Donor,sd) A:**Thr188** (3.46 Å) (Acceptor,sd) A:**Lys409** (2.93 Å) (Donor,sd)	7	A:**Trp110** (3.31 Å) A:Trp110 (3.48 Å)	A:**Arg78** (3.85 Å) (Carboxilate) A:**Lys409** (3.91 Å) (Carboxilate)
DA	5,491,963	−4.76	322.75	A:**Tyr74** (3.36 Å) (Acceptor,sd) A:**Glu292** (3.65 Å) (Donor,sd) A:**Glu292** (3.65 Å) (Acceptor,sd)	3	*Absent*	A:Arg71 (3.58 Å) (Carboxilate) A:**Lys409** (2.77 Å) (Carboxilate)
DG	151,148	−4.60	424.75	A:**Tyr74** (2.79 Å) (Acceptor,sd) A:**Tyr74** (2.38 Å) (Acceptor,sd) A:**Tyr74** (3.00 Å) (Donor,sd) A:**Ser186** (3.10 Å) (Donor,sd) A:**Lys409** (3.76 Å) (Acceptor,sd)	5	*Absent*	A:**Arg78** (4.39 Å) (Carboxilate) A:**Arg323** (4.91 Å) (Carboxilate) A:**Lys409** (3.28 Å) (Carboxilate) A:**Lys409** (3.81 Å) (Carboxilate)
EE	439,500	−6.21	27.93	A:**Tyr74** (3.75 Å) (Acceptor,sd) A:**Ser186** (3.02 Å) (Donor,sd) A:**Glu292** (3.06 Å) (Donor,sd) A:**Glu292** (3.06 Å) (Acceptor,sd)	4	A:**Tyr74** (3.42 Å) A:Trp110 (3.16 Å) A:Trp110 (3.02 Å)	A:Arg71 (3.50 Å) (Carboxilate) A:**Arg78** (3.65 Å) (Carboxilate) A:**Lys409** (4.16 Å) (Carboxilate) A:**Lys409** (3.40 Å) (Carboxilate)

Table 3. *Cont.*

Ligand	PubChem ID	Binding Energy (kcal/mol)	Inhibition Constant (μM)	Protein Residues Involved in H-Bond Interactions [Chain:Residue (Distance btw Donor-Acceptor) (Protein Donor/Acceptor, Residue from Side Chain)]	No. of H-Bonds	Protein Residues Involved in Hydrophobic Interactions [Chain:Residue (Distance btw Carbon Atoms)]	Protein Residues Involved in Salt Bridges [Chain:Residue (Distance btw Centers of Charge) (Ligand Functional Group Providing the Charge)]
ES	6,995,653	−4.17	875.75	A:**Tyr74** (2.82 Å) (Acceptor,sd) A:**Tyr74** (2.64 Å) (Acceptor,sd) A:**Ser186** (3.76 Å) (Donor,sd) A:**Asp318** (2.83 Å) (Accpetor,sd) A:Ser408 (4.07 Å) (Donor,sd) A:**Lys409** (3.00 Å) (Donor,sd)	6	A:**Tyr74** (3.70 Å) A:**Trp110** (3.30 Å)	A:**Lys409** (2.99 Å) (Carboxilate) A:**Lys409** (2.88 Å) (Carboxilate)
EV	6,992,567	−6.17	29.93	A:**Tyr74** (2.57 Å) (Acceptor,sd) A:**Tyr74** (3.86 Å) (Acceptor,sd) A:**Glu292** (2.53 Å) (Donor,sd) A:**Glu292** (2.53 Å) (Acceptor,sd)	4	A:**Trp110** (2.96 Å) A:**Glu292** (3.64 Å)	A:Arg71 (3.44 Å) (Carboxilate) A:**Lys409** (2.59 Å) (Carboxilate)
VG	6,993,111	−5.90	47.1	A:**Trp110** (2.96 Å) (Donor,sd) A:**Glu292** (2.57 Å) (Donor,sd) A:**Glu292** (2.57 Å) (Acceptor,sd)	3	A:**Tyr236** (3.83 Å) A:**Glu292** (3.92 Å)	A:Arg71 (3.50 Å) (Carboxilate)

Key residues of the binding site are highlighted in bold. Common residues for which glutamate and dipeptides interact are colored in purple.

DA (Asp-Ala)

DG (Asp-Gly)

EE (Glu-Glu)

ES (Glu-Ser)

EV (Glu-Val)

VG (Val-Gly)
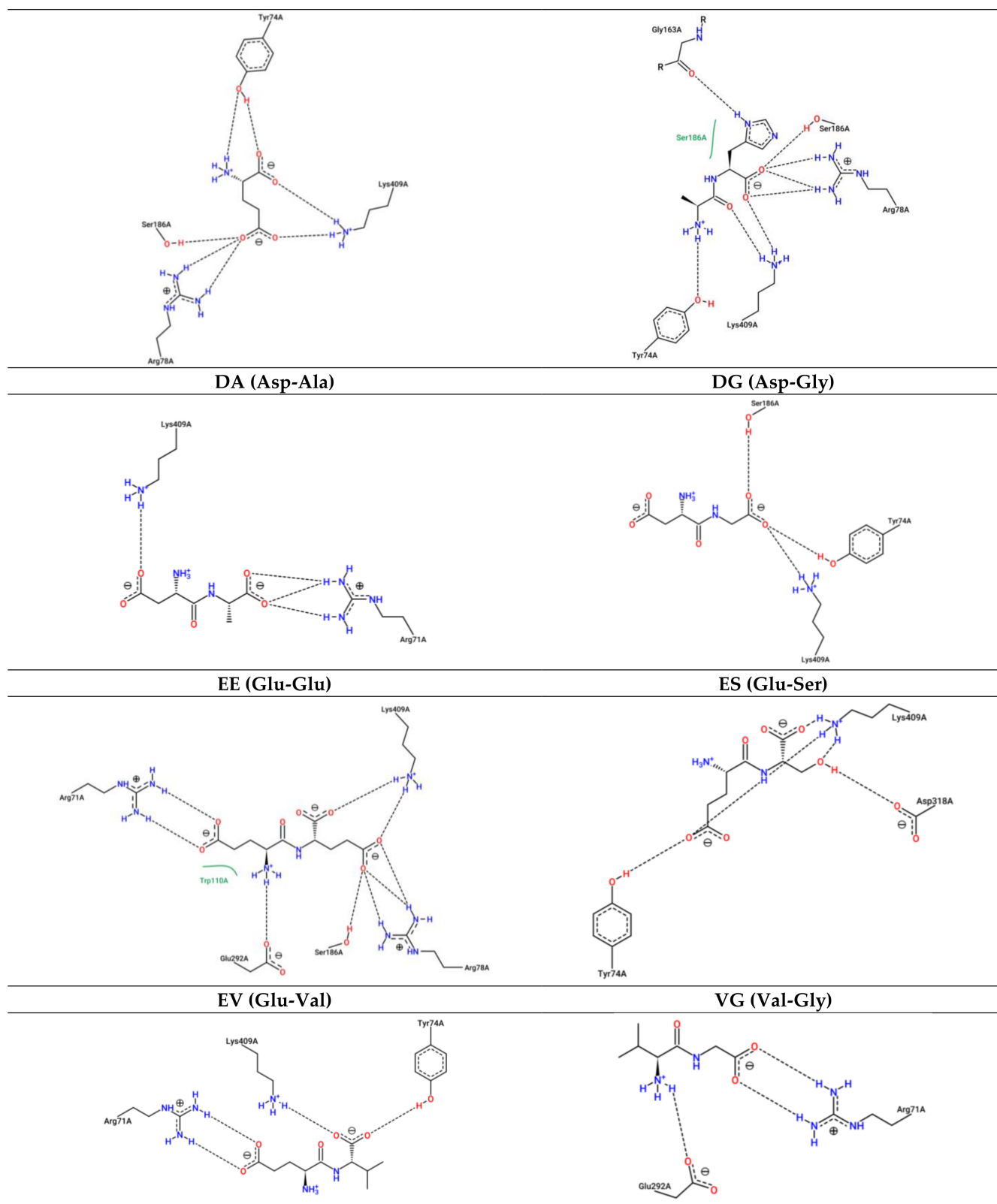
Figure 3. Two-dimensional representation of protein–ligand interactions between *Rattus norvegicus* open–open conformation of mGluR1 (PDB ID: 1EWT) and Glu (PubChem ID: 33032), AH (PubChem ID: 9837455), DA (PubChem ID: 5491963), DG (PubChem ID: 151148), EE (PubChem ID: 439500), ES (PubChem ID: 6995653), EV (PubChem ID: 6992567), VG (PubChem ID: 6993111). H bonds are shown as dashed lines, hydrophobic contacts are represented by green splines; the corresponding pocket residues are also shown in the same color. Diagrams obtained from the ProteinsPlus PoseView tool, from which E

amino acid was predicted to interact with Tyr74, Arg78, Ser186 and Lys409 by H-bonds; AH, with Tyr74, Arg78, Gly163, Ser186 and Lys409 by H-bonds and Ser186 by a hydrophobic interaction; DA, with Arg71 and Lys409 by H-bonds; DG, with Tyr74, Ser186, Lys409 by H-bonds; EE, with Arg71, Arg78, Ser186, Glu292 and Lys409 by H-bonds and Trp110 by hydrophobic interaction; ES, with Tyr74, Asp318 and Lys409 by H-bonds; EV, with Arg71, Tyr74 and Lys409 by H-bonds; and VG, with Arg71, and Glu292 by H-bonds.

Glutamic amino acid E (Ki = 694.05 μM) was revealed to stabilize bonds with *Rattus norvegicus* mGluR1 key receptor residues from open–open conformation Tyr74, Arg78, Ser186, and Lys409. Tyr74, Arg78, Ser165, Ser186, Thr188, and Lys409 were calculated for the case of the dipeptide AH (Ki = 12.32 μM). The dipeptide DA (Ki = 322.75 μM) would interact with key residues Tyr74, Glu292, and Lys409; while DG (Ki = 424.75 μM), with Tyr74, Arg78, Ser186, Arg323, and Lys409. E-containing dipeptide EE (Ki = 27.93 μM) was predicted to link to Tyr74, Arg78, Ser186, Glu292, and Lys409; whereas ES (Ki = 875.75 μM), with Tyr74, Ser186, Asp318, and Lys409; and EV (Ki = 29.93 μM) with Tyr74, Glu292 and Lys409. Finally, the dipeptide VG (Ki = 694.05 μM) was predicted to interact with key residues Glu292 and Tyr236. As in the previous case, more non-key residues seemed to be implicated in the stabilization of the dockings, such as Arg71 in DA, EE, EV, and VG; or Trp110 in AH, EE, ES, EV, and VG.

Receptor residues Tyr74 and Glu292 would be able to make H-bonds and hydrophobic forces, while Lys409 could form H-bonds and salt bridges in the same complex. Still, main interactions are due to H-bonds, highlighting the role of Tyr74, Ser186, and Glu292. Otherwise, the dipeptide AH, followed by ES, would make the greatest number of H-bonds, while in the case of the closed–open conformation, the peptides EE and ES reached a greater number of H-bonds. These differences may be due to the conformational changes of the receptor. Still, polar C-terminal amino acids may contribute to the establishment of H-bonds.

The number of salt bridges was greater than that of hydrophobic interactions in few cases, such as those from E and EE, while DA and DG lacked hydrophobic bonds.

The Ki values increased from AH, to EE, EV, VG, DA, DG, E, and finally, ES, which revealed that the Ki would not be benefited from the C-terminal non-polar residues, as it occurred in the closed–open conformation. As mentioned before, these differences may be due to the conformational changes, which would expose the key residues in a non-identical manner, translating it into different interactions and Ki values.

3.4. Interaction between Umami Dipeptides and Homo sapiens mGluR1 Open–Open Conformation

Results of these dockings are shown below by means of Table 4 and Figure 4.

Table 4. *Homo sapiens* open–open conformation (PDB ID: 3KS9) of mGluR1 residues involved in docking interactions with glutamic acid and the umami dry-cured ham dipeptides of this study, with docking scores.

Ligand	PubChem ID	Binding Energy (kcal/mol)	Inhibition Constant (µM)	Protein Residues Involved in H-Bond Interactions [Chain:Residue (Distance btw Donor-Acceptor) (Protein Donor/Acceptor, Residue from Side Chain)]	No. of H Bonds	Protein Residues Involved in Hydrophobic Interactions [Chain:Residue (Distance btw Carbon Atoms)]	Protein residues involved in Salt Bridges [Chain:Residue (Distance btw Centers of Charge) (Ligand Functional Group providing the Charge)]	π-Stacking [Chain:Residue (Distance in atm) (Stacking Type)]
E	33,032	−4.58	438.58	A:Tyr74 (2.49 Å) (Acceptor,sd) A:Tyr74 (2.74 Å) (Acceptor,sd) A:Tyr74 (2.42 Å) (Acceptor,sd) A:**Ser186** (3.17 Å) (Donor,sd)	4	A:Tyr74 (3.70 Å) A:**Trp110** (3.28 Å)	A:Arg78 (3.60 Å) (Carboxilate) A:Lys409 (2.59 Å) (Carboxilate) A:Lys409 (4.74 Å) (Carboxilate)	*Absent*
AH	9,837,455	−6.83	9.93	A:**Ser165** (2.96 Å) (Donor) A:**Ser186** (2.88 Å) (Acceptor) A:Thr188 (3.27 Å) (Donor,sd) A:Asn235 (2.78 Å) (Acceptor,sd) A:**Tyr236** (3.53 Å) (Donor) A:Thr188 (3.27 Å) (Acceptor,sd) A:Asp208 (3.73 Å) (Acceptor,sd) A:Gln211 (3.37 Å) (Donor,sd)	8	A:Thr188 (3.51 Å)	*Absent*	A:**Tyr236** (5.31 Å) (⊥)
DA	5,491,963	−5.50	92.95	A:**Ser165** (2.94 Å) (Donor) A:**Ser186** (2.58 Å) (Acceptor) A:**Ser186** (2.80 Å) (Acceptor) A:Thr188 (2.76 Å) (Donor) A:Thr188 (2.70 Å) (Acceptor,sd) A:Gln211 (3.44 Å) (Donor,sd) A:**Asp318** (2.91 Å) (Acceptor,sd)	7	A:Thr188 (3.22 Å)	A:Lys409 (3.58 Å) (Carboxilate)	*Absent*
DG	151,148	−4.82	294.68	A:**Ser165** (2.93 Å) (Donor) A:**Ser186** (3.99 Å) (Acceptor) A:**Ser186** (2.70 Å) (Acceptor) A:**Ser186** (2.98 Å) (Acceptor) A:Asp208 (3.83 Å) (Acceptor,sd)	5	A:Thr188 (3.25 Å)	A:Lys409 (3.25 Å) (Carboxilate)	*Absent*

Table 4. *Cont.*

Ligand	PubChem ID	Binding Energy (kcal/mol)	Inhibition Constant (μM)	Protein Residues Involved in H-Bond Interactions [Chain:Residue (Distance btw Donor-Acceptor) (Protein Donor/Acceptor, Residue from Side Chain)]	No. of H Bonds	Protein Residues Involved in Hydrophobic Interactions [Chain:Residue (Distance btw Carbon Atoms)]	Protein residues involved in Salt Bridges [Chain:Residue (Distance btw Centers of Charge) (Ligand Functional Group providing the Charge)]	π-Stacking [Chain:Residue (Distance in atm) (Stacking Type)]
EE	439,500	−4.92	248.83	A:**Ser165** (2.99 Å) (Donor) A:Ser186 (3.54 Å) (Donor,sd) A:Thr188 (2.68 Å) (Donor) A:Thr188 (2.87 Å) (Acceptor,sd) A:Thr188 (3.07 Å) (Acceptor,sd) A:Ser189 (3.87 Å) (Donor) A:Asp208 (3.25 Å) (Acceptor,sd) A:**Asp318** (2.92 Å) (Acceptor,sd)	8	A:Thr188 (3.03 Å) A:Leu342 (3.10 Å)	A:Lys409 (3.10 Å) (Carboxilate) A:Lys409 (3.28 Å) (Carboxilate)	*Absent*
ES	6,995,653	−5.16	165.54	A:**Ser165** (2.91 Å) (Donor) A:Thr188 (2.78 Å) (Acceptor,sd) A:Thr188 (2.79 Å) (Donor) A:Thr188 (2.67 Å) (Acceptor,sd) A:Thr188 (2.89 Å) (Acceptor,sd) A:Ser189 (4.07 Å) (Donor) A:Gln211 (3.73 Å) (Donor,sd) A:**Asp318** (3.88 Å) (Acceptor,sd)	8	A:Thr188 (3.40 Å) A:Leu342 (3.51 Å)	A:Lys409 (2.55 Å) (Carboxilate)	*Absent*
EV	6,992,567	−6.11	33.23	A:**Ser165** (3.02 Å) (Donor) A:Ser186 (2.89 Å) (Acceptor) A:Thr188 (2.62 Å) (Donor) A:Thr188 (2.68 Å) (Acceptor,sd) A:Thr188 (3.01 Å) (Acceptor,sd) A:Ser189 (3.86 Å) (Donor) A:Gln211 (3.87 Å) (Donor,sd) A:**Asp318** (3.13 Å) (Acceptor,sd)	8	A:Thr188 (2.97 Å) A:Leu342 (3.52 Å)	A:Lys409 (3.04 Å) (Carboxilate)	*Absent*
VG	6,993,111	−6.49	17.44	A:**Ser165** (3.02 Å) (Donor) A:Thr188 (2.80 Å) (Donor) A:Thr188 (2.83 Å) (Acceptor,sd) A:Thr188 (2.65 Å) (Acceptor,sd) A:Gln211 (3.24 Å) (Donor,sd) A:**Asp318** (2.86 Å) (Acceptor,sd)	6	A:Thr188 (3.28 Å) A:Leu342 (3.67 Å)	*Absent*	*Absent*

Key residues of the binding site are highlighted in bold. Common residues for which glutamate and dipeptides interact are colored in purple.

Figure 4. *Cont.*

EV (Glu-Val)	VG (Val-Gly)
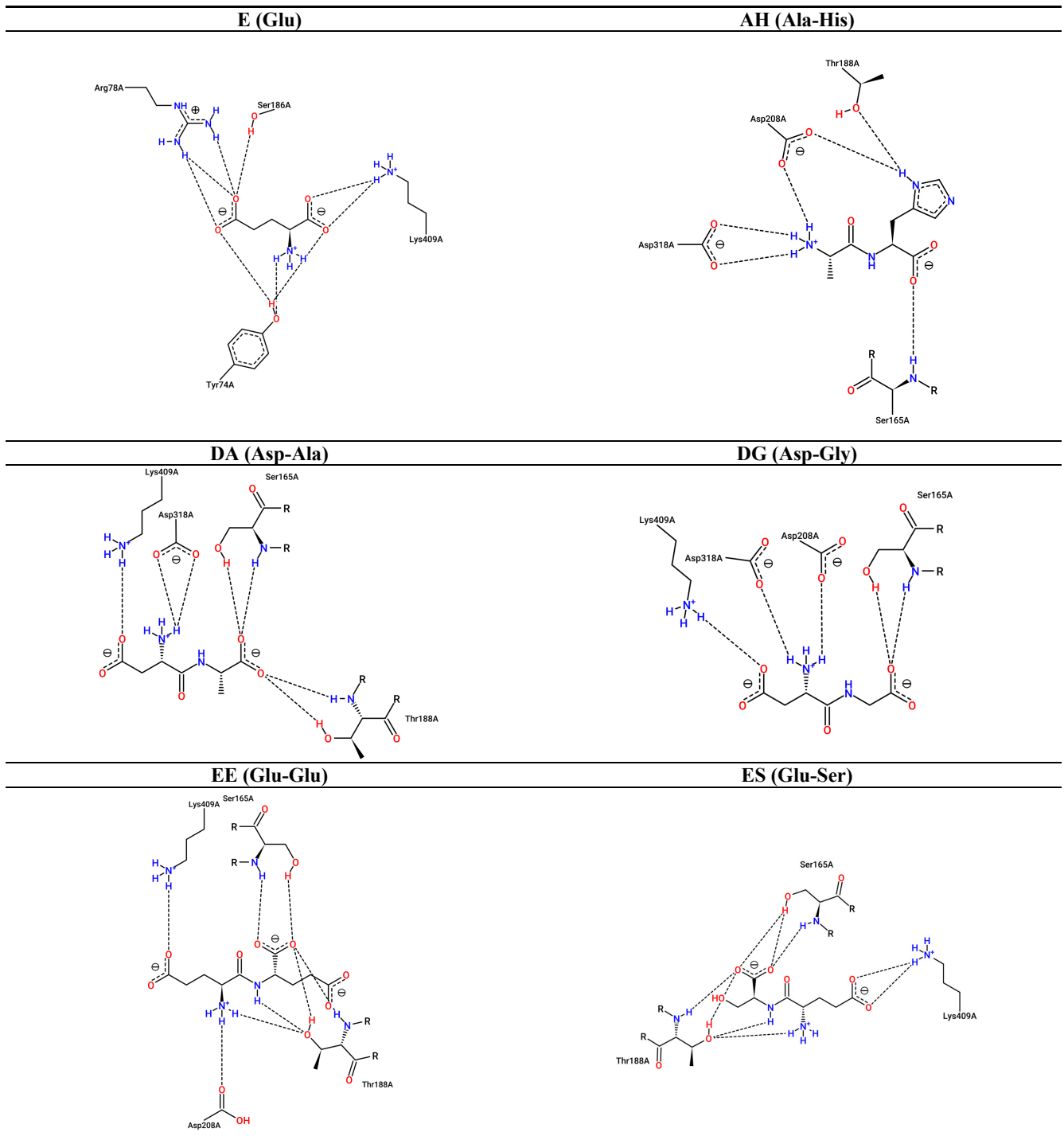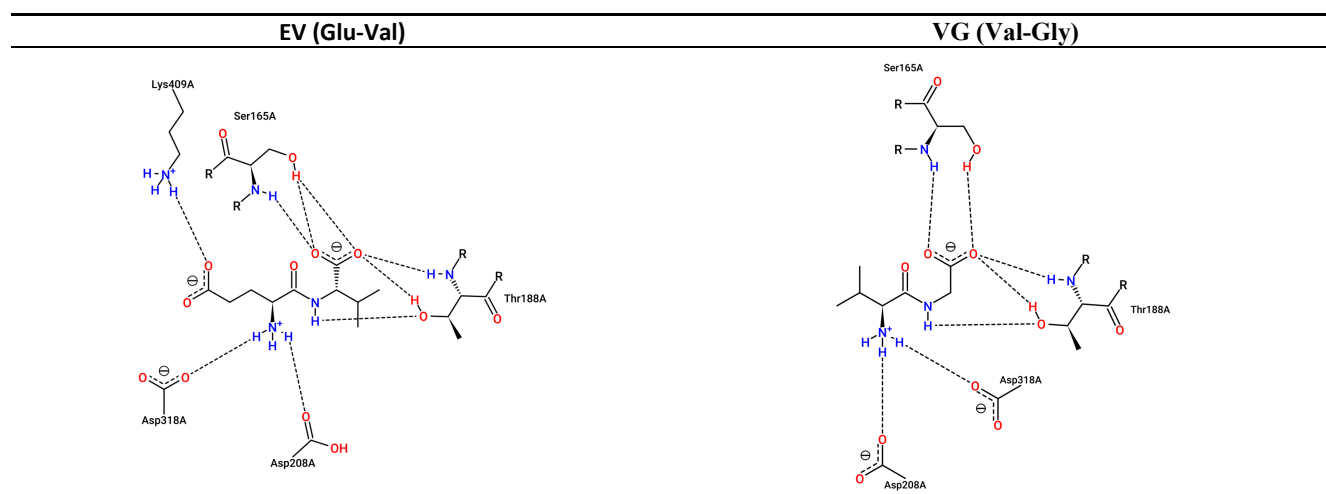
Figure 4. Two-dimensional representation of protein–ligand interactions between *Homo sapiens* open–open conformation of mGluR1 (PDB ID: 3KS9) and Glu (PubChem ID: 33032), AH (PubChem ID: 9837455), DA (PubChem ID: 5491963), DG (PubChem ID: 151148), EE (PubChem ID: 439500), ES (PubChem ID: 6995653), EV (PubChem ID: 6992567), VG (PubChem ID: 6993111). H bonds are shown as dashed lines, hydrophobic contacts are represented by green splines; the corresponding pocket residues are also shown in the same color. Diagrams obtained from the ProteinsPlus PoseView tool, from which E amino acid was predicted to interact with Tyr74, Arg78, Ser186, and Lys409; AH, with Ser165, Thr188, Asp208, Asp318; DA, with Ser165, Thr188, Asp318, and Lys409; DG, with Ser165, Asp208, Asp318 and Lys409; EE, with Ser165, Thr188, Asp208, and Lys409; ES, with Ser165, Thr188 and Lys409; EV, with Ser165, Thr188, Asp208, Asp318, and Lys409; and VG, with Ser165, Thr188, Asp208, and Asp318. H-bonds were estimated by PoseView to be stabilized in all cases.

According to Bupesh et al. (2016) [42], in the case of *Homo sapiens* mGluR1 open–open conformation docking, only their predicted key resides from the active site Trp110 and Ser186 would interact with E (Ki = 438.58 μM). AH could bond with Ser165, Ser186, and Tyr236. Intriguingly, it may not only stablish an H-bond with Tyr236, but also a perpendicular π-stacking interaction. With respect to DA (Ki = 92.95 μM), Ser165, Ser186, Asp318 would participate in the docking; it also happens in the case of EE (Ki = 248.83 μM), and EV (Ki = 33.23 μM). Whereas DG (Ki = 294.68 μM) could bind to Ser165 and Ser186, ES (Ki = 165.54 μM) and VG (Ki = 17.44 μM) would dock with Ser165 and Asp318. It is important to note that the repeatability of some non-key residues in all dipeptide cases, such as Thr188, Gln211, Lys409, and glutamic acid-binding residues Tyr74 and Arg78, suggest more of the previously predicted in the bibliography may be implicated in the recognition of umami compounds. Since the crystallographic structures 1EWK and 3KS9 are available in closed–open and open–open conformation states, the differences observed on residues may be due to conformational changes [64].

Apparently, residues, such as Thr188 and Tyr74, can form both H-bonds and hydrophobic interactions. However, as in the previous cases, most interactions are due to H-bonds. In fact, AH, EE, ES, and EV presented the same number of them with slightly differences in the residues implicated, which explains the diversity of Ki values and, thus, it may illustrate the receptor specificity. It seems that in the *Rattus norvegicus* closed–open conformation, polar acidic residues from dipeptides promote H-bonds. Salt bridges and hydrophobic connections appear to distribute differently compared to what occurred for the *Rattus norvegicus* mGluR1 receptor. Actually, the dipeptides AH and VG would not be able to stablish salt bridges.

Attending to the Ki, lower values were obtained for AH, EV, and VG. Making a comparison between the open–open conformations of *Rattus norvegicus* and *Homo sapiens*, the most frequent and common residues that interacted with E were Tyr74 and Lys409. This last residue is also remarkable for the case of dipeptides in joint with Ser186. However, a disparity of interactions between both receptors could be perceived, indicating that various key residues implicated in the recognition of the ligands would differ between the two

species although the sequence is highly conserved. Intriguingly, considering the residues predicted for the same receptor, the majority of them are repeated for each dipeptide. Indeed, the dipeptides may attach to the *Rattus norvegicus* closed–open conformation by Tyr74, Trp110, Ser186, Thr188, Asp318, Arg323, and Lys409. Tyr74, Trp110, Ser186, Glu292, and Lys409 frequently appeared for the case of *Rattus norvegicus* open–open conformation and Ser165, Ser186, Thr188, Gln211, Asp318, and Lys409 are remarkable attending to the *Homo sapiens* open–open conformation.

The open–open conformations from the two species generally presented lower number of H-bonds in comparison with the closed–open conformation from *Rattus norvegicus*, which probably was translated in a lower Ki value range. This may be because the conformational change to the closed form that occurred in the ligand-binding domain benefited the docking within the protomer, promoting a greater number of interactions. Based on the results provided by the in silico prediction, it seems the Ki did not show a particular trend attending to the peptide sequence as the dipeptides with lower values were not similar when comparing the cases. However, VG was present as one of those with the lowest Ki in all three cases.

There is little information reporting mechanism analyses with mGluR1. In fact, most investigations are based on the use of 1EWK and 3KS9 mGluR1s as templates for homology modeling to simulate the docking between drugs or taste-active molecules and T1R1/T1R3 or T2R1/T1R3 [65–70], and do not deepen the contribution of mGluRs to taste perception, although knockout studies have demonstrated that they play a key role independently of the heterodimers in umami recognition [29].

It is known that E recognition is accomplished by Tyr74, Arg78, Ser165, Ser186, Thr188, and Lys409 in both ligand-binding regions. However, residues Ser164, Asp208, Tyr236, Glu292, Gly293, Asp318, and Arg323, in the closed subunit, are implicated [62]. Some of these interactions were found in this study in both cases, but also when docking using the dipeptides as ligands. Docking simulations between 1EWK and sweet aspartyl-dipeptide derivatives revealed similar involved residues, such as Ser186, Asp318, and Lys409 through H-bonds; Arg78, Ser186, Thr188, Asp318, and Lys409 by salt bridges and Tyr74 and Tyr236 by hydrophobic interactions. In addition, some of the derivatives were able to stablish H-bonds with Trp110 and Gln211. The carboxylate groups appear to benefit the interaction with Lys409, whereas the carbonyl group ligand derivatives, with Arg323 as benzene ring-containing derivatives can have hydrophobic interactions with residues Tyr74 and Tyr236 [40]. Eugenol, a phenolic compound found in the leaves, buds, of clove *Syzygium aromaticum* (L.) Merrill and Perry, links with 3KS9 with similar residues, such as Trp110, Ser165, and Asp318 [42].

Such predicted estimations obtained in this study, in agreement with others, indicate that umami dipeptides dock the mGluR1 active site by mimicking E, but other residues may be implicated in each particular dipeptide to stabilize the binding.

Briefly, it is important to remark that these dipeptides have been previously demonstrated to exert bioactive properties. Indeed, the dipeptide AH has been registered on BioPep [71] as in vitro ACE-I and DPP-IV inhibitor and in vitro antioxidant. DA and DG can act as in vitro ACE-I inhibitors; DA can also act as in vitro DPP-III inhibitor. The dipeptide EE would act as a stimulating vasoactive substance release in human aortic endothelial cells; ES exerts in vitro DPP-IV inhibitory activity and EV and VG can be in vitro ACE and DPP-IV inhibitors.

More recently, dipeptides EE, ES, and DA have been tested for their anticholesterolemic activity obtaining values of 47.2, 45.5, and 49.6% of HMG-CoA inhibitory activity, respectively, at 1 mM [72].

On the other hand, as mentioned above, mGluR1 has been found in the stomach [27]. Specifically, it has been located at the apical membrane of chief cells and possibly in parietal cells in a rat glandular stomach. A diet with 1% E amino acid in rats was reported to induce changes in the expression of pepsinogen C and gastric intrinsic factor mRNAs in stomach mucosa [73], which suggests that mGluR1 is involved in the gastric phase regulation of

protein digestion [74]. Other genes affected by E supplementation were serotonin receptor 3A (*Htr3a*), nitric oxide synthase 3 (*Nos3*), phospholipase type C-β1 (*Plcb2*), and transient receptor potential cation channels *Trpc1* and *Trpm5*. The last three are related to the mGluR1 signal transduction cascade [73].

In addition, activation of mGluR1 modulates gastric vagal afferents from the luminal side, releasing mucin and nitrite mono-oxide, which stimulates serotonin (5HT) release at the enterochromaffin cell. Finally, this 5HT stimulates 5HT3 receptor at the nerve end of the vagal afferent fiber. Besides, studies in rats revealed that luminal E amino acid signaling contributes to control digestion and thermogenesis without obesity [75].

Thus, E amino acid-like tasting compounds, such as the dipeptides of this study, which are produced during the processing of dry-cured ham, might act as multifunctional agents, activating these responses by interaction with stomach mGluR1 [76].

4. Conclusions

The mGluR1 residues implicated in the recognition of E amino acid and umami dry-cured ham-derived dipeptides AH, DA, DG, EE, ES, EV, and VG, were, in silico, predicted through the use of *Rattus norvegicus* and *Homo sapiens* mGluR1 receptors for molecular docking. Results suggested that key residues from the binding site interact with E and dipeptides. However, other non-common residues may stabilize the dipeptide complex. Although differences in the residues implicated have been observed between mGluR1 of *Rattus norvegicus* and *Homo sapiens*, the most relevant residues were predicted to be Tyr74 and Lys409 for the recognition of E; and Ser186 and Lys409 for the docking of the dipeptides, being able to establish more than one bond and of different nature. Globally, AH and E-containing dipeptides seemed to make a greater number of H-bonds. In addition, no trend was detected when analyzing the Ki values, but VG was one of those presenting the lowest values. Finally, it is important to note that these umami compounds may play a role in digestion control and thermogenesis via stomach mGluR1. The results obtained here could provide information about sequence and taste relationships, and constitute a theoretical reference for the interactions of novel umami food-derived peptides.

References

1. Pérez-Santaescolástica, C.; Fraeye, I.; Barba, F.J.; Gómez, B.; Tomasevic, I.; Romero, A.; Moreno, A.; Toldrá, F.; Lorenzo, J.M. Trends in Food Science & Technology Application of Non-Invasive Technologies in Dry-Cured Ham: An Overview. *Trends Food Sci. Technol.* **2019**, *86*, 360–374. [CrossRef]
2. Toldrá, F.; Aristoy, M.C. Dry-Cured Ham. In *Handbook of Meat Processing*; John Wiley & Sons: Hoboken, NJ, USA, 2010; pp. 351–362. [CrossRef]
3. Carcò, G.; Schiavon, S.; Casiraghi, E.; Grassi, S.; Sturaro, E.; Bona, M.D.; Novelli, E.; L, G. Influence of Dietary Protein Content on the Chemico-Physical Profile of Dry-Cured Hams Produced by Pigs of Two Breeds. *Sci. Rep.* **2019**, 1–12. [CrossRef]
4. Bermúdez, R.; Franco, D.; Carballo, J.; Lorenzo, J.M. Physicochemical Changes during Manufacture and Final Sensory Characteristics of Dry-Cured Celta Ham. Effect of Muscle Type. *Food Control* **2014**, *43*, 263–269. [CrossRef]
5. Tomažin, U.; Škrlep, M.; Prevolnik, M.; Batorek, N.; Karolyi, D. The Effect of Salting Time and Sex on Chemical and Textural Properties of Dry Cured Ham. *Meat Sci.* **2020**, *161*, 107990. [CrossRef] [PubMed]
6. Čandek-Potokar, M.; Škrlep, M. Factors in Pig Production That Impact the Quality of Dry-Cured Ham: A Review. *Animal* **2012**, 327–338. [CrossRef] [PubMed]
7. Mora, L.; Gallego, M.; Escudero, E.; Reig, M.; Aristoy, M.C.; Toldrá, F. Small Peptides Hydrolysis in Dry-Cured Meats. *Int. J. Food Microbiol.* **2015**, *212*, 9–15. [CrossRef]
8. Mora, L.; Bolumar, T.; Heres, A.; Toldrá, F. Effect of Cooking and Simulated Gastrointestinal Digestion on the Activity of Generated Bioactive Peptides in Aged Beef Meat. *Food Funct.* **2017**, *8*. [CrossRef] [PubMed]
9. Toldrá, F.; Flores, M.; Sanz, Y. Dry-Cured Ham Flavour: Enzymatic Generation and Process Influence. *Food Chem.* **1997**, *59*, 523–530. [CrossRef]
10. Toldrá, F.; Flores, M. The Role of Muscle Proteases and Lipases in Flavor Development during the Processing of Dry-Cured Ham. *Crit. Rev. Food Sci. Nutr.* **1998**, *38*, 331–352. [CrossRef] [PubMed]
11. Toldrá, F.; Gallego, M.; Reig, M.; Aristoy, M.-C.; Mora, L. Bioactive Peptides Generated in the Processing of Dry-Cured Ham. *Food Chem.* **2020**, *321*, 126689. [CrossRef]
12. Aristoy, M.-C.; Toldrá, F. Isolation of Flavor Peptides from Raw Pork Meat and Dry-Cured Ham. *Dev. Food Sci.* **1995**, *37*, 1323–1344. [CrossRef]
13. Sakurai, T.; Misaka, T.; Nagai, T.; Ishimaru, Y.; Matsuo, S.; Asakura, T.; Abe, K. PH-Dependent Inhibition of the Human Bitter Taste Receptor HTAS2R16 by a Variety of Acidic Substances. *J. Agric. Food Chem.* **2009**, *57*, 2508–2514. [CrossRef]
14. Kim, M.J.; Son, H.J.; Kim, Y.; Misaka, T.; Rhyu, M.-R. Umami–Bitter Interactions: The Suppression of Bitterness by Umami Peptides via Human Bitter Taste Receptor. *Biochem. Biophys. Res. Commun.* **2015**, *456*, 586–590. [CrossRef]
15. Sentandreu, M.A.A.; Stoeva, S.; Aristoy, M.C.C.; Laib, K.; Voelter, W.; Toldra, E.; Toldrá, F.; Toldra, E. Identification of Small Peptides Generated in Spanish Dry-Cured Ham. *J. Food Sci.* **2003**, *68*, 64–69. [CrossRef]
16. Jamkhande, P.G.; Ghante, M.H.; Ajgunde, B.R. Software Based Approaches for Drug Designing and Development: A Systematic Review on Commonly Used Software and Its Applications. *Bull. Fac. Pharmacy, Cairo Univ.* **2017**, *55*, 203–210. [CrossRef]
17. Pak, V.V.; Koo, M.; Kwon, D.Y.; Yun, L. Design of a Highly Potent Inhibitory Peptide Acting as a Competitive Inhibitor of HMG-CoA Reductase. *Amino Acids* **2012**, *43*, 2015–2025. [CrossRef]
18. Pant, S.; Singh, M.; Ravichandiran, V.; Murty, U.S.N.; Srivastava, H.K. Peptide-like and Small-Molecule Inhibitors against Covid-19. *J. Biomol. Struct. Dyn.* **2021**, *39*, 2904–2913. [CrossRef] [PubMed]
19. Zhang, X.; Qiao, L.; Chen, Y.; Zhao, B.; Gu, Y.; Huo, X.; Zhang, Y.; Li, G. In Silico Analysis of the Association Relationship between Neuroprotection and Flavors of Traditional Chinese Medicine Based on the MGluRs. *Int. J. Mol. Sci.* **2018**, *19*, 163. [CrossRef] [PubMed]
20. Iwaniak, A.; Minkiewicz, P.; Darewicz, M.; Protasiewicz, M.; Mogut, D. Chemometrics and Cheminformatics in the Analysis of Biologically Active Peptides from Food Sources. *J. Funct. Foods* **2015**, *16*, 334–351. [CrossRef]
21. Iwaniak, A.; Minkiewicz, P.; Darewicz, M.; Hrynkiewicz, M. Food Protein-Originating Peptides as Tastants - Physiological, Technological, Sensory, and Bioinformatic Approaches. *Food Res. Int.* **2016**, *89*, 27–38. [CrossRef]
22. Finger, T.E. ATP Signaling Is Crucial for Communication from Taste Buds to Gustatory Nerves. *Science* **2005**, *310*, 1495–1499. [CrossRef]
23. Yoshida, R.; Shigemura, N.; Sanematsu, K.; Yasumatsu, K.; Ishizuka, S.; Ninomiya, Y. Taste Responsiveness of Fungiform Taste Cells With Action Potentials. *J. Neurophysiol.* **2006**, *96*, 3088–3095. [CrossRef] [PubMed]
24. Shirazi-Beechey, S.P.; Daly, K.; Al-Rammahi, M.; Moran, A.W.; Bravo, D. Role of Nutrient-Sensing Taste 1 Receptor (T1R) Family Members in Gastrointestinal Chemosensing. *Br. J. Nutr.* **2014**, *111*, S8–S15. [CrossRef]
25. Chaudhari, N.; Landin, A.M.; Roper, S.D. A Metabotropic Glutamate Receptor Variant Functions as a Taste Receptor. *Nat. Neurosci.* **2000**, *3*, 113–119. [CrossRef] [PubMed]
26. Gabriel, A.S.; Uneyama, H.S.Y.; Torii, K. Cloning and Characterization of a Novel MGluR1 Variant from Vallate Papillae That Functions as a Receptor for L-Glutamate Stimuli. *Chem. Senses* **2005**, *30* (Suppl. 1), i25–i26. [CrossRef] [PubMed]
27. San Gabriel, A.M. Taste Receptors in the Gastrointestinal System. *Flavour* **2015**, *4*, 14. [CrossRef]
28. Nelson, G.; Chandrashekar, J.; Hoon, M.A.; Feng, L.; Zhao, G.; Ryba, N.J.P.; Zuker, C.S. An Amino-Acid Taste Receptor. *Nature* **2002**, *416*, 199–202. [CrossRef]

29. Kusuhara, Y.; Yoshida, R.; Ohkuri, T.; Yasumatsu, K.; Voigt, A.; Hübner, S.; Maeda, K.; Boehm, U.; Meyerhof, W.; Ninomiya, Y. Taste Responses in Mice Lacking Taste Receptor Subunit T1R1. *J. Physiol.* **2013**, *591*, 1967–1985. [CrossRef]

30. Delay, E.R.; Hernandez, N.P.; Bromley, K.; Margolskee, R.F. Sucrose and Monosodium Glutamate Taste Thresholds and Discrimination Ability of T1R3 Knockout Mice. *Chem. Senses* **2006**, *31*, 351–357. [CrossRef]

31. Kim, S.; Chen, J.; Cheng, T.; Gindulyte, A.; He, J.; He, S.; Li, Q.; Shoemaker, B.A.; Thiessen, P.A.; Yu, B.; et al. PubChem 2019 Update: Improved Access to Chemical Data. *Nucleic Acids Res.* **2019**, *47*, D1102–D1109. [CrossRef]

32. Natesh, R.; Schwager, S.L.U.; Sturrock, E.D.; Acharya, K.R. Crystal Structure of the Human Angiotensin-Converting Enzyme–Lisinopril Complex. *Nature* **2003**, *421*, 551–554. [CrossRef]

33. Dobrovetsky, E.; Khutoreskaya, G.; Seitova, A.; Cossar, D.; Edwards, A.M.; Arrowsmith, C.H.; Bountra, C.; Weigelt, J.; Bochkarev, A. Metabotropic Glutamate Receptor Mglur1 Complexed with LY341495 Antagonist. **2010**. Unpublished.

34. Berman, H.M. The Protein Data Bank. *Nucleic Acids Res.* **2000**, *28*, 235–242. [CrossRef]

35. Morris, G.M.; Huey, R.; Lindstrom, W.; Sanner, M.F.; Belew, R.K.; Goodsell, D.S.; Olson, A.J. AutoDock4 and AutoDockTools4: Automated Docking with Selective Receptor Flexibility. *J. Comput. Chem.* **2009**, *30*, 2785–2791. [CrossRef]

36. Sanner, M.F. Python: A Programming Language for Software Integration and Development. *J. Mol. Graph. Model.* **1999**, *17*, 57–61.

37. Fährrolfes, R.; Bietz, S.; Flachsenberg, F.; Meyder, A.; Nittinger, E.; Otto, T.; Volkamer, A.; Rarey, M. ProteinsPlus: A Web Portal for Structure Analysis of Macromolecules. *Nucleic Acids Res.* **2017**, *45*, W337–W343. [CrossRef] [PubMed]

38. Salentin, S.; Schreiber, S.; Haupt, V.J.; Adasme, M.F.; Schroeder, M. PLIP: Fully Automated Protein–Ligand Interaction Profiler. *Nucleic Acids Res.* **2015**, *43*, W443–W447. [CrossRef] [PubMed]

39. Volkamer, A.; Kuhn, D.; Grombacher, T.; Rippmann, F.; Rarey, M. Combining Global and Local Measures for Structure-Based Druggability Predictions. *J. Chem. Inf. Model.* **2012**, *52*, 360–372. [CrossRef]

40. Muchtaridi, M.; Amir, S.F.B.; Indriyati, W.; Musfiroh, I. Interaction of Aspartyl-Dipeptides Derivatives with Metabotropic Glutamate Receptor (MGluR) Using Molecular Docking Simulation. *Res. J. Pharm. Biol. Chem. Sci.* **2015**, *6*, 478–485.

41. Belenikin, M.S.; Baskin, I.I.; Costantino, G.; Palyulin, V.A.; Pellicciari, R.; Zefirov, N.S. Comparative Analysis of the Ligand-Binding Sites of the Metabotropic Glutamate Receptors MGluR1–MGluR8. *Dokl. Biochem. Biophys.* **2002**, *386*, 251–256. [CrossRef]

42. Bupesh, G.; Meenakumari, K.; Prabhu, J.; Prabhu, K.; Kalaiselvi, V.S.; Manikandan, E.; Krishnarao, M.R.; Sathyarajeswaran, P. Molecular Properties and Insilico Neuroprotective Activity of Eugenol Against Glutamate Metabotrophic Receptors. *Int. J. Pharm. Sci. Rev. Res.* **2016**, *40*, 318–323.

43. Adasme, M.F.; Linnemann, K.L.; Bolz, S.N.; Kaiser, F.; Salentin, S.; Haupt, V.J.; Schroeder, M. PLIP 2021: Expanding the Scope of the Protein–Ligand Interaction Profiler to DNA and RNA. *Nucleic Acids Res.* **2021**. [CrossRef]

44. Schöning-Stierand, K.; Diedrich, K.; Fährrolfes, R.; Flachsenberg, F.; Meyder, A.; Nittinger, E.; Steinegger, R.; Rarey, M. ProteinsPlus: Interactive Analysis of Protein–Ligand Binding Interfaces. *Nucleic Acids Res.* **2020**, *48*, W48–W53. [CrossRef] [PubMed]

45. Toldrá, F.; Gallego, M.; Reig, M.; Aristoy, M.-C.; Mora, L. Recent Progress in Enzymatic Release of Peptides in Foods of Animal Origin and Assessment of Bioactivity. *J. Agric. Food Chem.* **2020**, *68*, 12842–12855. [CrossRef] [PubMed]

46. Sentandreu, M.; Toldrá, F. Evaluation of ACE Inhibitory Activity of Dipeptides Generated by the Action of Porcine Muscle Dipeptidyl Peptidases. *Food Chem.* **2007**, *102*, 511–515. [CrossRef]

47. Panchaud, A.; Affolter, M.; Kussmann, M. Mass Spectrometry for Nutritional Peptidomics: How to Analyze Food Bioactives and Their Health Effects. *J. Proteomics* **2012**, *75*, 3546–3559. [CrossRef]

48. Mora, L.; Gallego, M.; Reig, M.; Toldrá, F. Challenges in the Quantitation of Naturally Generated Bioactive Peptides in Processed Meats. *Trends Food Sci. Technol.* **2017**, *69*, 306–314. [CrossRef]

49. Takahashi, K.; Tokuoka, M.; Kohno, H.; Sawamura, N.; Myoken, Y.; Mizuno, A. Comprehensive Analysis of Dipeptides in Alcoholic Beverages by Tag-Based Separation and Determination Using Liquid Chromatography/Electrospray Ionization Tandem Mass Spectrometry and Quadrupole-Time-of-Flight Mass Spectrometry. *J. Chromatogr. A* **2012**, *1242*, 17–25. [CrossRef]

50. Tang, Y.; Li, R.; Lin, G.; Li, L. PEP Search in MyCompoundID: Detection and Identification of Dipeptides and Tripeptides Using Dimethyl Labeling and Hydrophilic Interaction Liquid Chromatography Tandem Mass Spectrometry. *Anal. Chem.* **2014**, *86*, 3568–3574. [CrossRef]

51. Dang, Y.; Gao, X.; Ma, F.; Wu, X. Comparison of Umami Taste Peptides in Water-Soluble Extractions of Jinhua and Parma Hams. *LWT - Food Sci. Technol.* **2015**, *60*, 1179–1186. [CrossRef]

52. Wang, J.; Zhao, G.M.; Zhang, J.W.; Liu, Y.X.; Li, M.Y.; Hu, D.H. Separation, Purification and Structural Identification of Small Peptides from Jinhua Ham. *Food Sci.* **2012**, *33*, 16–20. [CrossRef]

53. Zhu, C.-Z.; Tian, W.; Li, M.-Y.; Liu, Y.-X.; Zhao, G.-M. Separation and Identification of Peptides from Dry-Cured Jinhua Ham. *Int. J. Food Prop.* **2017**, *20* (Suppl. 3), S2980–S2989. [CrossRef]

54. Zhou, C.-Y.; Tang, C.-B.; Wang, C.; Dai, C.; Bai, Y.; Yu, X.-B.; Li, C.-B.; Xu, X.-L.; Zhou, G.-H.; Cao, J.-X. Insights into the Evolution of Myosin Light Chain Isoforms and Its Effect on Sensory Defects of Dry-Cured Ham. *Food Chem.* **2020**, *315*, 126318. [CrossRef] [PubMed]

55. Gallego, M.; Mora, L.; Aristoy, M.C.; Toldrá, F. Titin-Derived Peptides as Processing Time Markers in Dry-Cured Ham. *Food Chem.* **2015**, *167*, 326–339. [CrossRef]

56. Gupta, S.; Kapoor, P.; Chaudhary, K.; Gautam, A.; Kumar, R.; Raghava, G.P.S. In Silico Approach for Predicting Toxicity of Peptides and Proteins. *PLoS One* **2013**, *8*, e73957. [CrossRef] [PubMed]

57. Altschul, S.F.; Gish, W.; Miller, W.; Myers, E.W.; Lipman, D.J. Basic Local Alignment Search Tool. *J. Mol. Biol.* **1990**, *215*, 403–410. [CrossRef]

58. Tharmalingam, S.; Burns, A.R.; Roy, P.J.; Hampson, D.R. Orthosteric and Allosteric Drug Binding Sites in the Caenorhabditis Elegans Mgl-2 Metabotropic Glutamate Receptor. *Neuropharmacology* **2012**, *63*, 667–674. [CrossRef]

59. Crupi, R.; Impellizzeri, D.; Cuzzocrea, S. Role of Metabotropic Glutamate Receptors in Neurological Disorders. *Front. Mol. Neurosci.* **2019**, *12*. [CrossRef]

60. San Gabriel, A.; Maekawa, T.; Uneyama, H.; Torii, K. Metabotropic Glutamate Receptor Type 1 in Taste Tissue. *Am. J. Clin. Nutr.* **2009**, *90*, 743S–746S. [CrossRef]

61. Nango, E.; Akiyama, S.; Maki-Yonekura, S.; Ashikawa, Y.; Kusakabe, Y.; Krayukhina, E.; Maruno, T.; Uchiyama, S.; Nuemket, N.; Yonekura, K.; et al. Taste Substance Binding Elicits Conformational Change of Taste Receptor T1r Heterodimer Extracellular Domains. *Sci. Rep.* **2016**, *6*, 25745. [CrossRef] [PubMed]

62. Kunishima, N.; Shimada, Y.; Tsuji, Y.; Sato, T.; Yamamoto, M.; Kumasaka, T.; Nakanishi, S.; Jingami, H.; Morikawa, K. Structural Basis of Glutamate Recognition by a Dimeric Metabotropic Glutamate Receptor. *Nature* **2000**, *407*, 971–977. [CrossRef]

63. Stierand, K.; Maass, P.C.; Rarey, M. Molecular Complexes at a Glance: Automated Generation of Two-Dimensional Complex Diagrams. *Bioinformatics* **2006**, *22*, 1710–1716. [CrossRef]

64. Chen, Q.; Ho, J.D.; Ashok, S.; Vargas, M.C.; Wang, J.; Atwell, S.; Bures, M.; Schkeryantz, J.M.; Monn, J.A.; Hao, J. Structural Basis for (S)-3,4-Dicarboxyphenylglycine (DCPG) As a Potent and Subtype Selective Agonist of the MGlu 8 Receptor. *J. Med. Chem.* **2018**, *61*, 10040–10052. [CrossRef]

65. López Cascales, J.J.; Oliveira Costa, S.D.; de Groot, B.L.; Walters, D.E. Binding of Glutamate to the Umami Receptor. *Biophys. Chem.* **2010**, *152*, 139–144. [CrossRef] [PubMed]

66. Liu, H.; Da, L.-T.; Liu, Y. Understanding the Molecular Mechanism of Umami Recognition by T1R1-T1R3 Using Molecular Dynamics Simulations. *Biochem. Biophys. Res. Commun.* **2019**, *514*, 967–973. [CrossRef] [PubMed]

67. Zhang, F.; Klebansky, B.; Fine, R.M.; Liu, H.; Xu, H.; Servant, G.; Zoller, M.; Tachdjian, C.; Li, X. Molecular Mechanism of the Sweet Taste Enhancers. *Proc. Natl. Acad. Sci.* **2010**, *107*, 4752–4757. [CrossRef]

68. Raliou, M.; Grauso, M.; Hoffmann, B.; Schlegel-Le-Poupon, C.; Nespoulous, C.; Debat, H.; Belloir, C.; Wiencis, A.; Sigoillot, M.; Preet Bano, S.; et al. Human Genetic Polymorphisms in T1R1 and T1R3 Taste Receptor Subunits Affect Their Function. *Chem. Senses* **2011**, *36*, 527–537. [CrossRef] [PubMed]

69. Yu, Z.; Kang, L.; Zhao, W.; Wu, S.; Ding, L.; Zheng, F.; Liu, J.; Li, J. Identification of Novel Umami Peptides from Myosin via Homology Modeling and Molecular Docking. *Food Chem.* **2021**, *344*, 128728. [CrossRef] [PubMed]

70. Dang, Y.; Hao, L.; Cao, J.; Sun, Y.; Zeng, X.; Wu, Z.; Pan, D. Molecular Docking and Simulation of the Synergistic Effect between Umami Peptides, Monosodium Glutamate and Taste Receptor T1R1/T1R3. *Food Chem.* **2019**, *271*, 697–706. [CrossRef] [PubMed]

71. Minkiewicz, P.; Iwaniak, A.; Darewicz, M. BIOPEP-UWM Database of Bioactive Peptides: Current Opportunities. *Int. J. Mol. Sci.* **2019**, *20*, 5978. [CrossRef] [PubMed]

72. Heres, A.; Mora, L.; Toldrá, F. Inhibition of 3-Hydroxy-3-Methyl-Glutaryl-Coenzyme A Reductase Enzyme by Dipeptides Identified in Dry-Cured Ham. *Food Prod. Process. Nutr.* **2021**, *3*, 18. [CrossRef]

73. San Gabriel, A.M.; Maekawa, T.; Uneyama, H.; Yoshie, S.; Torii, K. MGluR1 in the Fundic Glands of Rat Stomach. *FEBS Lett.* **2007**, *581*, 1119–1123. [CrossRef] [PubMed]

74. Zhang, J.; Yin, Y.; Shu, X.G.; Li, T.; Li, F.; Tan, B.; Wu, Z.; Wu, G. Oral Administration of MSG Increases Expression of Glutamate Receptors and Transporters in the Gastrointestinal Tract of Young Piglets. *Amino Acids* **2013**, *45*, 1169–1177. [CrossRef]

75. Torii, K.; Uneyama, H.; Nakamura, E. Physiological Roles of Dietary Glutamate Signaling via Gut–Brain Axis Due to Efficient Digestion and Absorption. *J. Gastroenterol.* **2013**, *48*, 442–451. [CrossRef] [PubMed]

76. Kondoh, T.; Mallick, H.N.; Torii, K. Activation of the Gut-Brain Axis by Dietary Glutamate and Physiologic Significance in Energy Homeostasis. *Am. J. Clin. Nutr.* **2009**, *90*, 832S–837S. [CrossRef] [PubMed]